J Mol Model (2012) 18:3627–3637
DOI 10.1007/s00894-012-1364-9

ORIGINAL PAPER

Transportation behavior of alkali ions through a cell membrane ion channel. A quantum chemical description of a simplified isolated model

Ferenc Billes · Ildikó Mohammed-Ziegler · Hans Mikosch

Received: 3 November 2011 / Accepted: 17 January 2012 / Published online: 22 February 2012

Abstract Quantum chemical model calculations were carried out for modeling the ion transport through an isolated ion channel of a cell membrane. An isolated part of a natural ion channel was modeled. The model channel was a calixarene derivative, hydrated sodium and potassium ions were the models of the transported ion. The electrostatic potential of the channel and the energy of the channel-ion system were calculated as a function of the alkali ion position. Both attractive and repulsive ion-channel interactions were found. The calculations – namely the dependence of the system energy and the atomic charges of the water molecules with respect to the position of the alkali ion in the channel – revealed the molecular-structural background of the potassium selectivity of this artificial ion channel. It was concluded that the studied ion channel mimics real biological ion channel quite well.

Keywords Channel potential · Hydrated ion · Infrared spectrum · Ion channel · Ion channel interaction · Quantum chemistry

F. Billes
Department of Physical Chemistry,
Budapest University of Technology and Economics,
H-1521 Budapest Budafoki út 8.,
Hungary
e-mail: fbilles@mail.bme.hu

I. Mohammed-Ziegler (✉)
Hemercy KKT,
H-2521 Arany Janos u. 28.,
Csolnok, Hungary
e-mail: mohazihu@yahoo.com

F. Billes · H. Mikosch
Institute for Chemical Technologies and Analytics,
Vienna University of Technology,
A-1060 Vienna, Getreidemarkt 9/164/EC,
Austria

H. Mikosch
e-mail: Hans.Mikosch@tuwien.ac.at

Present Address:
I. Mohammed-Ziegler
Gedeon Richter Plc,
H-2510 Esztergomi út 27.,
Dorog, Hungary
e-mail: mohammedne@richter.hu

Introduction

Ion channels are – by definition – pore-forming proteins that help to establish and control the small voltage gradient across the plasma membrane of cells by allowing the flow of ions down their electrochemical gradient [1]. Transport of alkali metals, particularly sodium and potassium, across cell membranes is an essential function with exceptional selectivity. Ion channels, e.g., mediate conduction across nerves, thus they are especially prominent components of the nervous system. They are typically involved in rapid changes in cells, and therefore ion channels are key components in a wide variety of biological processes, such as cardiac, skeletal, and smooth muscle contraction, epithelial transport of nutrients and ions, T-cell activation, etc. Understanding the mechanism of their actions is an important step in finding efficient treatments for diseases in which ion channel malfunctions are recognized. In the search for new drugs, ion channels are frequently targeted [1–3].

Till now, the properties of ion channels were studied mainly experimentally [1–4] in their original, biological environment, i.e., in living organisms. For instance, a nanomagnetometric study was published by Hall et al. [5], representing the state-of-the-art. However, among *in vitro* observations there are two main approaches for gaining further insight into the working

mechanism of these channels. One opportunity is to apply different quantum chemical methods in order to find out the structural properties of biological molecules at atomic-molecular level. The other option is to model the functioning of natural ion channels by artificially built molecular structures.

The results of *in silico* studies are really diverse. Recently more attention is also paid to their modeling using both classical methods [6] and quantum chemical methods. Guidoni and Carloni [7], for instance, modeled a potassium channel of an unicellar organism combining quantum chemistry with molecular mechanics (QC/MM). Roux [8] studied the structure of Gramicidin A by solid NMR and molecular dynamics simulations. Grigorenko et al. applied effective fragment potential for cell membrane systems [9]. Vogel's electronic research note gave a short survey on modeling of transport across biological membranes with several references [10]. Simulation of ion current through natural ion channels based on classical and quantum chemical considerations is further developed (see, e.g., [11]). Abad et al. [12] observed narrow ion channels. Poznanski and Bell dealt with the theoretical analysis of the amplification of synaptic potentials by small clusters of persistent sodium channels in dendrites [13, 14]. Chen, Tsai and Chen studied a Markov model for the problem of ion channel modeling [15]. Reviews on the structure-function relationship of natural ion channels were published by Ash et al. [16] and Tieleman et al. [17].

As was mentioned above, the second option is to mimic the natural ion transport system by artificial models and then to compare the properties of the models with those of the natural ones. As known, cell membranes are built up from lipid double layers. Each layer consists of a series of parallel oriented molecules with a relatively small polar head and one (or more) long non-polar alkyl chain(s). The polar heads are directed toward the membrane surfaces while the non-polar chains turn toward each other (Fig. 1). The ion channels have to form a tube for the ion transport. Therefore, the polar head of the model molecule has to have an orifice, and at least three long alkyl chains must be attached at the same side of the head.

Earlier, Bohmer [18] described that feature of calixarenes, in particular calix[4]arene, that they had potential cation filters since they were readily functionalized on both upper and lower rims. Calix[4]arenes have a second property which can be exploited to make ion channels: they exist in different conformers which can, in some cases, be interconverted. If a symmetric filter is required it can be constructed from a cone conformer, however, an asymmetric compound can be prepared from the 1,4-alternate conformer.

Kobuke [19, 20] (after constructing the first non-peptide ion channel) built both a cation selective and voltage dependent artificial ion channel consisting of two resorcinarene molecules. This active molecular assembly was proven to be potassium selective (with a 3x factor over sodium ion) resembling that of Gramicidin A. Conduction of sodium ion could be blocked by addition of rubidium ions. Conductance was not observed by analogous compounds prepared with shorter substituents leading the authors to speculate that the compounds inserted in phospholipid layers exhibited cation transport when two molecules met 'tail-to-tail'. When cholic acid derivatives of the resorcin[4]arene were inserted in the bilayer

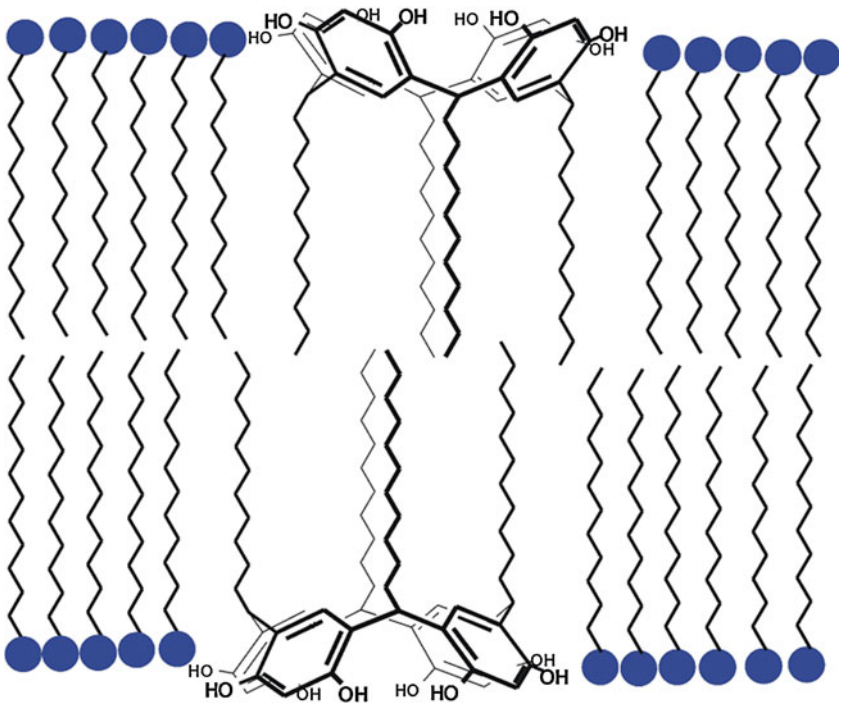

Fig. 1 Model of a cell membrane

structure, the model gave channels with longer open state lifetimes without affecting the K^+-selectivity.

Analogous artificial channel was constructed recently by Kulikov et al. [21] based on a gall[4]arene molecule substituted with four dodecyl chains (one on each methanediyl bridge) and embedded in phospholipid bilayer succesfully.

In this work, the properties of Kobuke's [19, 20] artificial isolated ion channel were studied: 2,8,14,20-tetra-n-undecyl-4,6,10,12,16,18,22,24-octahydroxycalix[4]arene (tetraundecylresorcinarene, TUR, see Fig. 2) was the model molecule. The transported ion was modeled by a hydrated sodium ion and a potassium one, respectively. We aimed to characterize the structural background of the ion selectivity of the molecular assembly containing TUR at the molecular level and to compare these properties with those of natural ion channels. In the construction of our model, the capacity of the applied computer had to be taken into account, therefore a simplified model was analyzed in this manner.

Experimental section

Compound. 2,8,14,20-tetra-n-undecyl-4,6,10,12,16,18,22,24-octahydroxycalix[4]arene (CAS number 112247-07-1) was purchased from Aldrich (as monohydrate, 99.10 % of purity) and applied without any further purification.

Infrared spectra were recorded on a Nicolet Magna 750 FT-IR spectrometer in KBr pellet at 1 cm^{-1} of resolution by accumulating 512 scans.

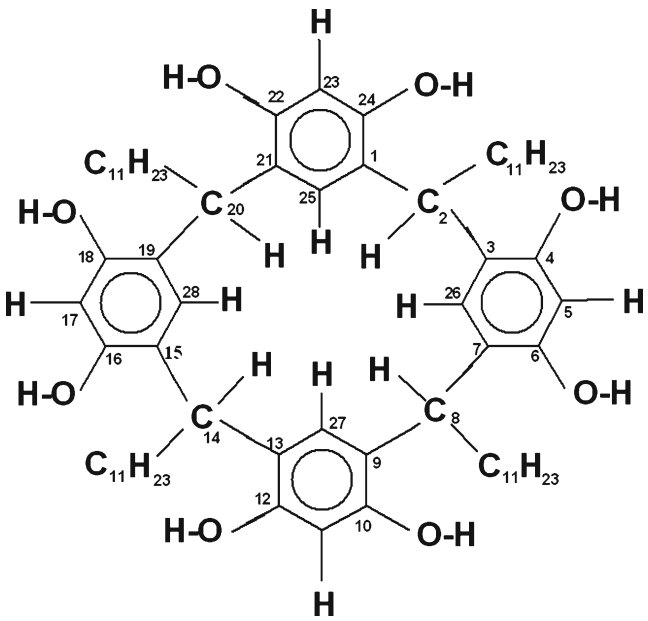

Fig. 2 The intramolecular connections in 2,8,14,20-tetra-n-undecyl-4,6,10,12,16,18,22,24-octahydroxycalix[4]arene

Calculation methods

With the choice of our model we had to take into consideration our quantum chemical possibilities. These restricted the size of the model molecule, the quantum chemical method and the medium of the environment. Regarding the very large TUR molecule (it contains 192 atoms), the quantum chemical calculations were restricted to the semiempirical level and to the isolated (in vacuum) molecule. A semiquantitative description of the ion transport process is possible under these conditions. The Gaussian 98 program package was applied with the semiempirical AM1 method [22]. The limit for the molecular orbitals made it impossible to treat the complete model ion channel in the calculations together with the surrounding membrane chemical structure, therefore the computation was restricted to the isolated TUR molecule.

The *first step* of the calculations was the geometry optimization. The input geometry was based on our earlier results on 25,26,27,28-tetrahydroxicalix[4]arene [23]. For a better handling of the molecule, the four n-undecyl chains were turned into their all-trans conformation. The result of the computation was transformed into a coordinate system with the molecular symmetry axis as one of the coordinate axes (stressed axis, with arbitrary zero, see Fig. 4, double TUR). In this step the fundamental frequencies and the infrared intensities were computed as well. The obtained data were used for the calculation of the simulated infrared spectrum.

The collective effect of the channel atoms on the transported ion can be expressed by the electrostatic potential function along the symmetry axis. Therefore the *second step* of our work was the calculation of the electrostatic potential in a large region along the direction of the stressed axis beyond both ends of the molecule. The calculated potential was practically constant at the end of the undecyl chains and also beyond the ends. Therefore, it was possible to arrange two TUR molecules with their apolar feet toward each other and, to construct the potential function along the full ion channel axis by simple fitting.

For the ion transport calculations, the geometric parameters of the Na^++$2H_2O$ and K^++$2H_2O$ complexes were also necessary. The optimized r_e geometry of this system was calculated using DFT Becke3P86 functional and the 6-311 G(d,p) basis set [22]. At the same time, the fundamental frequencies and the infrared intensities were also computed and from these entries, the simulated infrared spectrum was obtained.

The ion channel interactions were followed by AM1 single point calculations pushing forward the ions along the symmetry axis of the channel. The system energy and the atomic net charges of the water part of the Na^++$2H_2O$ and K^++$2H_2O$ clusters (subsystems) were computed as a function of the alkali ion positions. The single point calculations were computed

with 0.5 Å steps, and, where the energy function changed rapidly, with 0.25 Å steps.

Results and discussion

Geometry of TUR

The computed optimized geometry is presented in Fig. 3. According to these results, the molecular symmetry is not C_{4v} as was expected from Fig. 2 but its symmetry is only $C_{2v.}$ This is in good agreement with our earlier calculations for 25,26,27,28-tetrahydroxicalix[4]arene [23–26]. The oxygen atoms form two zones in the –16.55 to -16.45 Å and in the –14.50 to –14.40 Å regions of the stressed axis (Fig 4). The corresponding H atoms of the OH groups are situated in the –17.45 to –17.40 and in the –14.85 to –14.75 Å regions. The molecule is placed between –17.75 and -1.25 Å. On the second (Fig. 4, right) half of the ion channel, one can find that the corresponding positions are symmetrical with positive sign.

Comparing our results with those obtained by Mäkinen et al. [27], there are significant differences. In the literature calculations for this resorcinarene showed extensive intramolecular H-bonds and a C_{4v} structure. Moreover, the saddle conformer prevents the formation H-bonds between resorcinarene molecules in this paper [27]. However, C_{4v} geometry was resulted because the H-bonded structures were modeled as planar conformers in equilibrium state and fixed during the calculations. In our calculations it was obviously not the case since the alkyl groups exhibit repulsion that prevents the formation of tubular structure.

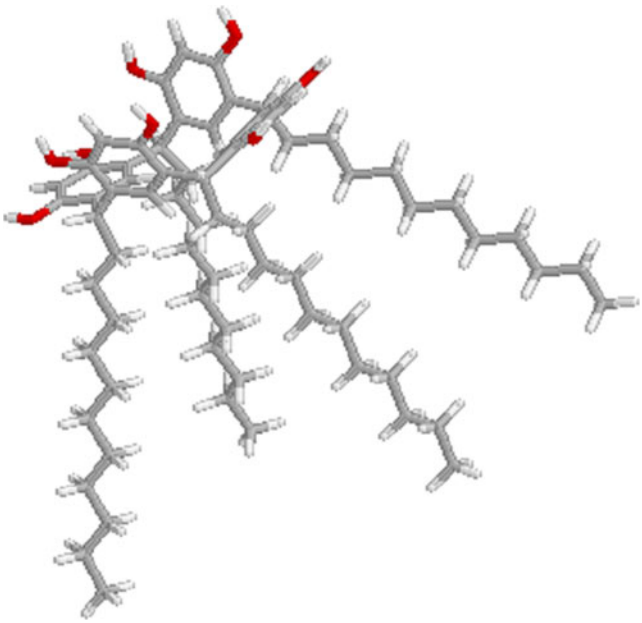

Fig. 3 The AM1 calculated geometry of 2,8,14,20-tetra-n-undecyl-4,6,10,12,16,18,22,24-octahydroxycalix[4]arene

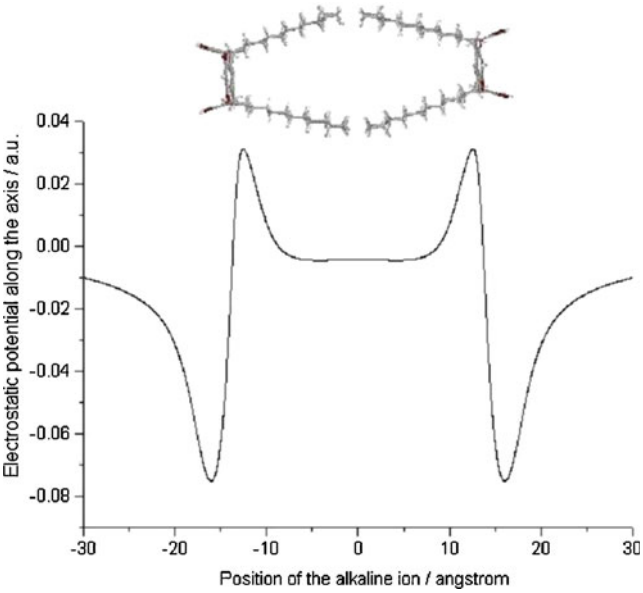

Fig. 4 The electrostatic potential along the symmetry axis of the 2,8,14,20-tetra-n-undecyl-4,6,10,12,16,18,22,24-octahydroxycalix[4]arene molecule

The C_{2v} geometry is the result of the freely moving molecular structure during the calculations.

Electrostatic potential along the ion channel

The calculated electrostatic potential is shown in Fig. 4. The effect of the OH groups is already observable at a long distance from these groups, from about –25 Å up to -6.0 Å. At the channel entrance, a very strong attractive potential can act on the ions, its maximum value is –0.07524 Hartree/a.u. (a.u.: atomic charge unit, absolute value of the electron charge) at –16.08 Å. Deeper in the channel, the attraction changes to repulsion at a maximum at –12.53 Å with 0.03130 Hartree/a.u. The source of this extremum is the repulsive effect of the hydrogen atoms of hydrocarbon chains toward the alkali ion. However, this repulsion decreases with the **dilatation of the tubular structure of hydrocarbon chains.** The potential reaches its initial value again at about -6.0 Å, afterward it remains practically constant. That means, the polar part of the molecule has a very large effect even far from the OH groups. The attractive interactions are mainly due to the repulsion between the M^+ (M: metal) and the oxygen atoms carrying partial negative charges. However, the cation-pi interactions at the mouth of the channel also contribute, since those carbon atoms of the resorcinarene which are directed toward the channel carry negatively charged.

IR spectrum of TUR

Recorded and simulated infrared spectra are compared in Fig. 5. For the simulation, Lorentzian band shapes were applied with 15 cm^{-1} of FWHH. The size of the molecule made impossible the scaling of the calculated force constants based on the chemical properties of the internal coordinates. The definition of the necessary 570 internal coordinates and the work with matrices of 570×570 size prevented us from this type of scaling. Therefore we multiplied the calculated frequencies with a common 0.92 scale factor. Frequencies higher than 3300 cm^{-1} were not affected by scaling.

The measured spectrum clearly shows the interactions of TUR. This compound forms practically infinite quantity of intermolecular hydrogen bonds, since each TUR molecule contains 12 hydroxyl groups. The very strong and broad OH band between 3600 and 3100 cm^{-1} reflects these interactions. Comparing the measured and simulated spectra, it is clear that hydrogen bonds exist only in condensed state, i.e., such intermolecular interactions are not present in the isolated molecule (i.e., this molecule is vacuum) since the OH groups are far from each other (as apparent from the comparison of the OH stretching bands in the 3600-3100 cm^{-1}, and the bending modes in the 1600-1100 cm^{-1} regions).

Theoretically it is possible that intramolecular H-bonds are also formed. However, for this the solid undecyl resorcinarene should be arranged close to planar-structured conformers (see, e.g., Mäkinen et al. [27]). However, in the studied and modeled, freely rotating structure the hydroxyl groups corresponding to different resorcinol moieties are relatively far from each other (8,2-8,3 Å) therefore the formation of intramolecular hydrogen bonds is hindered. Therefore it can be concluded that under the studied conditions, intermolecular hydrogen bonds are not formed.

The hydrated sodium and potassium ions

It is well-known that alkali ions coordinates four water molecule in the solid state. However, Rempe and Pratt [28] observed the energetics of hydrated alkali ions with maximum four water molecules while moving along an ion channel and found that protein functional groups stabilize both sodium and potassium ions by replacing their first inner shell water molecules (with equal favor). That means a substantial contribution to ion channel selectivity arises from thermodynamic features of exchange between the hydrated ion ligands and carbonyl or other functional groups on the ion channel wall. Actually, alkali ions hydrated by four water molecules are too large compared to the pore size of the TUR molecule in spite of the fact that ion transport through this ion channel was experimentally justified [19, 20]. Therefore in our model, the alkali ions were hydrated by two water molecules instead of the maximal four.

As was expected, bihydrated sodium and potassium ions exist in C_{2v} symmetry. Figure 6 shows their *structure*, Table 1 contains their optimized r_e geometric parameters. Comparing the geometric parameters of the two complexes, considerable difference exists only between the alkali ion-

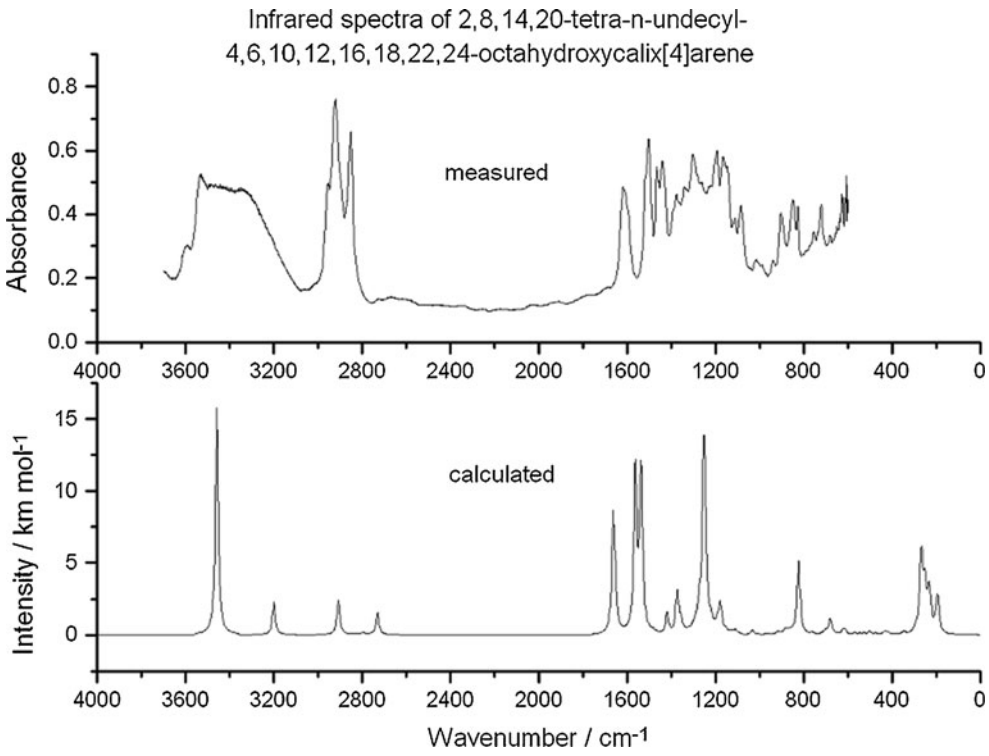

Fig. 5 Measured and calculated infrared spectra of 2,8,14,20-tetra-n-undecyl-4,6,10,12,16,18,22,24-octahydroxycalix[4]arene

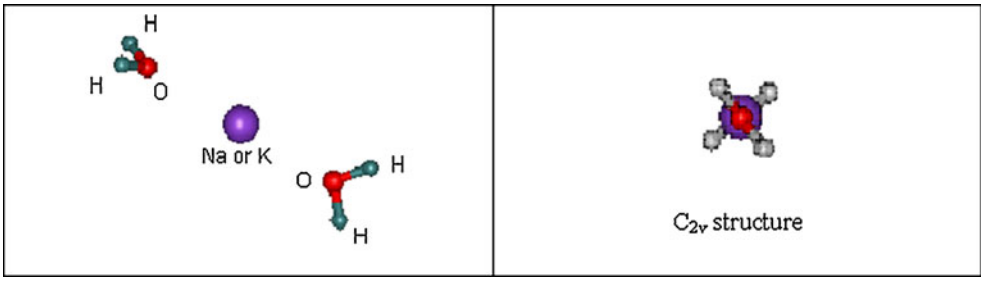

Fig. 6 The calculated structures of the Na^++$2H_2O$ and K^++$2H_2O$ complexes

oxygen distances. This is a consequence of the differences in the ionic radii (see Table 3). Table 2 presents the net atomic charges of the optimized structures. It is interesting that the atomic net charge of both the Na^+ and the K^+ ions is less than one a.u.. Considering the greater ion-oxygen distance, the effect of the potassium ion on the water molecules is less than in the case of sodium ion. Therefore, the potassium ion remains more positive than the sodium cation in hydrated state, and its influence on the water molecules is less. Consequently, the oxygen atom has less negative, and the hydrogen ion has less positive charge in the K^++$2H_2O$ complex than in the Na^++$2H_2O$ system.

The artificial ion channel

Our ion channel model is set aside from the environment existing in a living cell. Therefore we describe it semiquantitatively. Thus, it has to be kept in mind that the calculated energy, charge and potential values introduce the living ion channel properties in the frame of our approximation mainly in their tendencies.

The structure of the ion channel and the electrostatic potential along its symmetry axis are presented in Fig 4. As was mentioned above, the channel was calculated by fitting of two TUR molecules. The distance between the nonpolar feet of the two molecules was chosen as 2.5 Å. The TUR molecule on the right side was rotated around its symmetry axis by 45º to the left for the simulation of the possible random positions of the molecules in the real cell membrane. This rotation, however, has no influence on the electrostatic potential energy at the symmetry axis. The potential function is, therefore, symmetric: the graph of the function on the right side of the molecule is a mirror image of that of the left side of the molecule. The function has minima at –16.33 and at 16.33 Å, both with –0.07524 Hartree/a.ch.u. The two maxima are at –12.78 Å and at 12.78 Å, both with 0.03130 Hartree/a.ch.u. (Fig. 7). Consequently, the oxygen atoms of the bihydrated ions form four zones with extreme values in the –16.55 to -16.45, the –14.50 to –14.40, 14.40 to 14.50 and 16.40 to 16.50 Å regions of the symmetry axis (Fig. 8). The corresponding H atoms of the OH groups are situated in the –17.45 to –17.40, –14.85 to –14.75, 14.75 to 14.85 and 17.40 to 17.45 Å regions (Fig. 9).

In our calculations, the polar head of the TUR molecule on the left side of the channel was regarded as input for the ions. This molecule was placed between –17.75 and –1.25 Å. According to this model, the polar head of the molecule on the right side is the channel output. This molecule is situated between 1.25 and 17.75 Å (output).

Ion transport

The *alkali ion* transport is characterized by the change of the system energy (TUR+subsystem complex) during its movement along the symmetry axis of the channel. This function has maxima at about –12.53 Å on the stressed coordinate (entrance region of the channel) and at about 12.53 Å (exit region of the channel) both of them with -0.5330 Hartree. Figures 7, 8, and 9 show the potential function in comparison with several other functions depending on the type and position of alkali ion.

The dehydrated sodium and potassium ions show very strong interactions with the active zones while crossing the polar heads of the channel (Fig. 7). Two potential maxima at

Table 1 Optimized geometric parameters of the Na^++$2H_2O$ and K^++$2H_2O$ complexes[a]

Parameter Na^++$2H_2O$	Optimized value[b]	Parameter K^++$2H_2O$	Optimized value[b]
Na-O	2.268	K-O	2.606
O-H	0.963	O-H	0.962
Na-H	2.812	K-H	3.196
Na-O-H	127.5	K-O-H	127.8
H-O-H	105.1	H-O-H	104.4

[a] Becke3P86/6-311G(d,p) calculations

[b] Distances are expressed in angstroms, and angles in degrees

Table 2 Atomic net charges in the Na^++$2H_2O$ and K^++$2H_2O$ complexes[a]

Atom	Net charge (a.u.)	Atom	Net charge (a.u.)
Na^+	0.8265	K^+	0.8737
all O	−0.5403	all O	−0.5371
all H	0.3135	all H	0.3001

[a] Becke3P86/6-311G(d,p) calculations

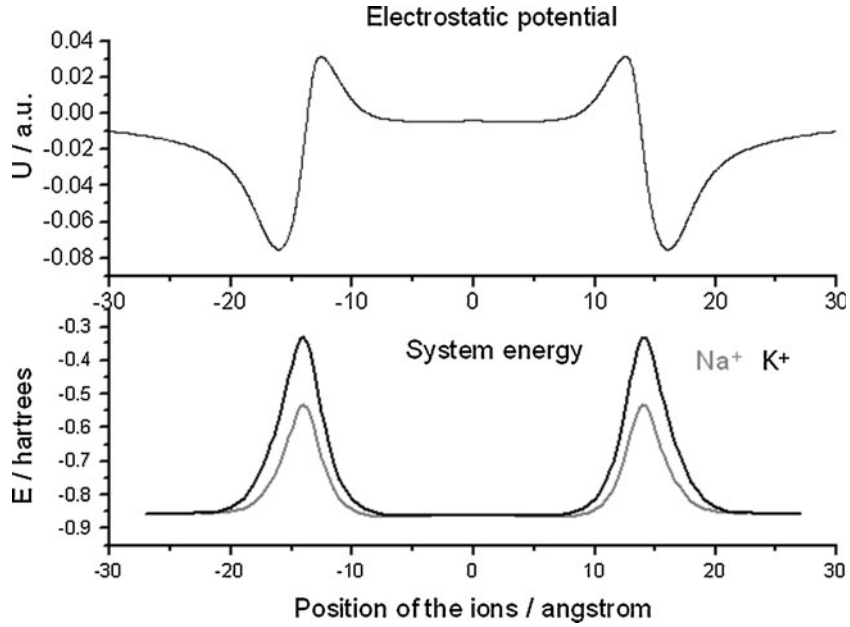

Fig. 7 Electrostatic potential and system energies with Na^+ and K^+ ions along the symmetry axis of the ion channel

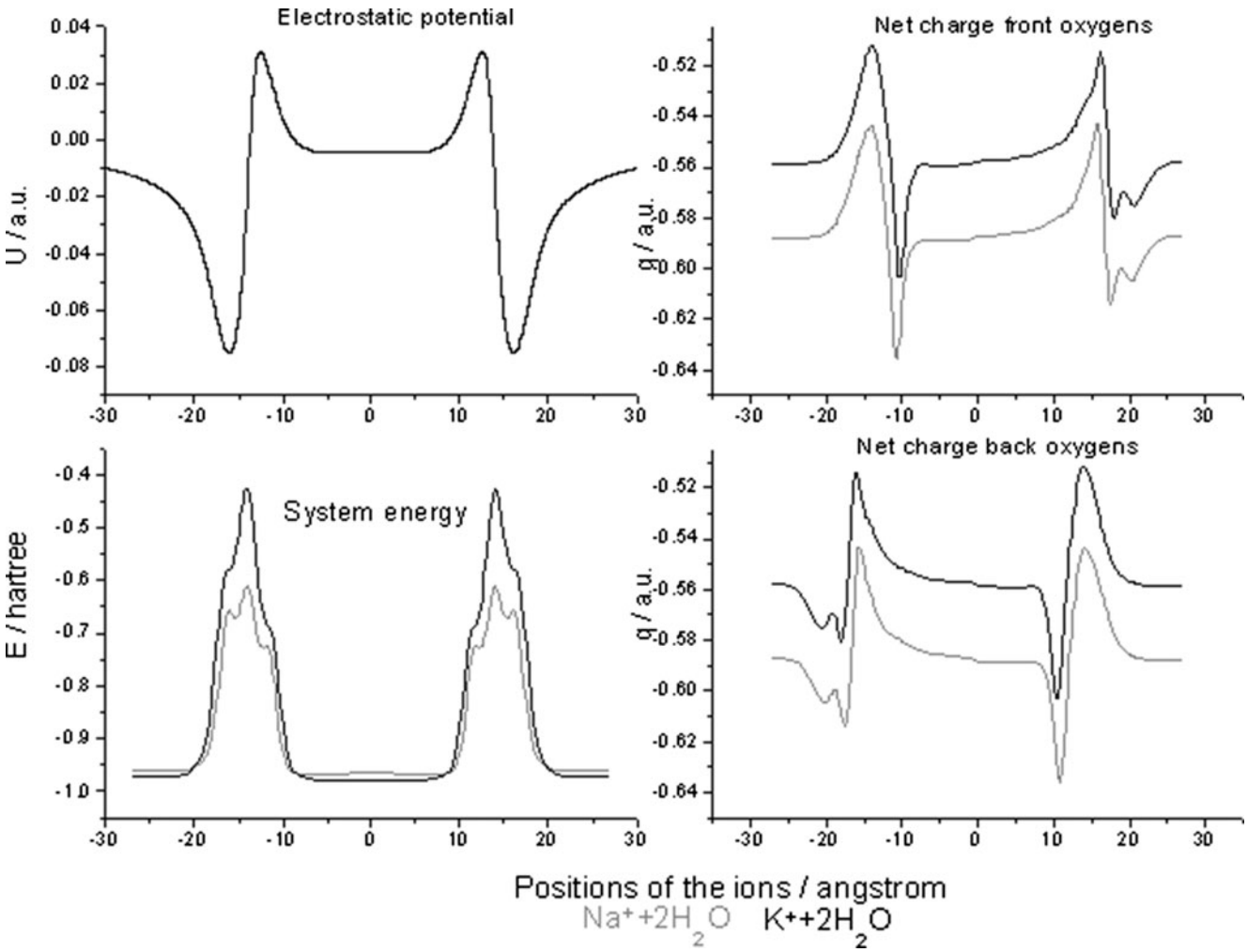

Fig. 8 Electrostatic potential, molecular energies and *oxygen* net charges of the $Na^+ + 2H_2O$ and $K^+ + 2H_2O$ complexes along the symmetry axis of the ion channel

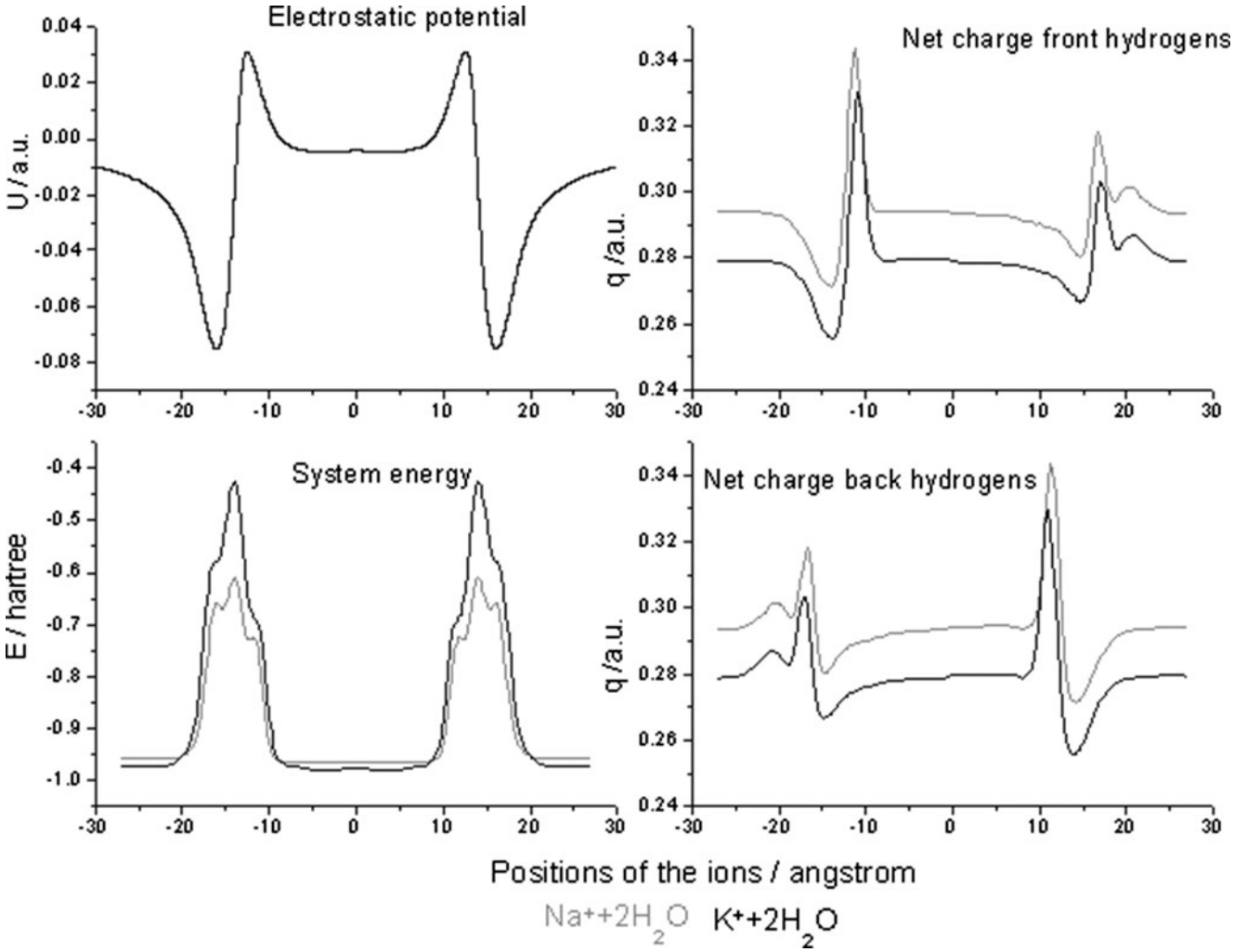

Fig. 9 Electrostatic potential, molecular energies and *hydrogen* net charges of the Na^++2H_2O and K^++2H_2O complexes along the symmetry axis of the ion channel

about –14.0 and +14 Å are resulted. These maxima can be found between the minima and maxima of the potential curve. The positions of the maxima are independent of the chemical nature of the ion, however, the interaction with the potassium ion is stronger.

The energy functions of the *bihydrated alkali ion* transport through the ion channel are rather complex. The moving complex consists of five different parts while interacting with the atoms of the channel. At the front of the moving system, there are the hydrogen atoms of a water molecule, behind them the front oxygen atom is positioned, the alkali ion is located in the middle of the complex. It is followed by the oxygen atom of the back water molecule and at the tail there are the back hydrogens of this molecule. These five parts cross the active zones of the channel at different positions of the alkali ions. For illustration, the geometric parameters of the subsystems are presented in Table 2. The total length of the sodium complex is about 5.6 Å, while that of the potassium is 6.2 Å.

The energy function of the hydrated ions has three maxima in each half of the channel; i.e., altogether six (Figs. 8 and 9). Theoretically, more maxima may exist, since all seven atoms of the subsystems may interact with all the atoms of all channel hydroxyl groups. However, as it was mentioned above, there are only two oxygen and two hydroxyl hydrogen zones in a half channel and only the H…O and Na…O (K…O) interactions are strong. In this way, some interactions overlap. The energy maxima with the Na^++2H2O complex are -0.6575 Hartree (at ±15.75 Å), -0.6158 Hartree (at ±14.00 Å) and a shoulder with –0.7255 Hartree (at ±11.50 Å). The interactions with the K^++2H_2O complex are also substantially stronger here than those with the hydrated sodium ion. However, only two maxima were observed with –0.4262 Hartree at ±14.00 Å and two shoulders at about ±15.50 Å ±11.50 Å. The last one is only slightly observable (see Fig. 8). The maxima at ±14.0 Å have the same positions as in the case of dehydrated ions but the channel-ion interactions are shielded here by the water

Table 3 Some results on the structure optimizations of alkali ions in the artifical ion channel

Ion	Input position[a]	Optimized position[a]	Displacement[a]	Net ionic charge[b]	Net ionic charge[c]	Ionic radius[d]
Li^+	−17.500	−14.278	3.222	1.071	1.071	0.600
Na^+	−17.500	−18.647	−1.147	1.000	1.000	0.950
K^+	−17.500	−10.179	7.321	1.000	1.000	1.330
Rb^+	−17.500	−16.960	0.540	1.000	1.000	1.480
Li^+	−13.000	−11.959	1.041	1.113	1.113	0.600
Na^+	−13.000	−6.174	6.826	1.000	1.000	0.950
K^+	−13.000	−4.324	8.676	1.000	1.000	1.330
Rb^+	−13.000	−12.352	0.648	1.000	1.000	1.480

[a]See Fig. 4 for the channel axis coordinate, angstroms

[b]Mulliken's atomic net charges, a.u

[c]Mulliken's net charges, those of joined atoms summed to that of the heavy atom

[d]Pauli's ionic radii, angstroms

molecules, and therefore they are weaker. The two other maxima / shoulders reflect the channel-water interactions.

As was mentioned above, the net charges of the alkali ions in optimized structure of the bihydrated alkali complexes is less than one (Table 2). However, during the transports along the ion channel, the alkali ion charges are found to always be one.

It is interesting to follow the changes in the atomic net charges of the water molecules along the channel. Although the complexes are symmetric, from the point of view of the motion along the channel, they are not equivalent. We have to distinguish front and back water molecules. Besides, the hydrogen atoms in the front are before the oxygen, while on the back side the order is opposite.

The net charges of the front *oxygen* atoms have maxima at –14.00 Å, –15.70 Å and beyond the exit at 18.75 Å. The minima were found at –10.75 Å, 17.50 Å and beyond the channel exit at 20.25 Å. For the back oxygen atoms, all the maxima and minima were observed with opposite sign. The positions of these extrema refer to the oxygen atoms of both sodium and potassium complexes.

The charge functions of the front and back *hydrogen atoms* of the hydrated complexes are somewhat different. There are small differences in the charges of hydrogen atom pairs of the same water molecule. This fact reflects their slightly different chemical environment. Their obtained average charge functions are presented in Fig. 9. At the entrance of the channel, the front hydrogen meets the polar head of the TUR and moves along the apolar part of the molecule. By moving forward the aqueous ion-complex "feels" the field of the apolar part of the second TUR and by crossing through, the polar zone reaches the exit. The situation of the front and back hydrogens is similar with regard to the effect of the oxygens of the hydrated ions.

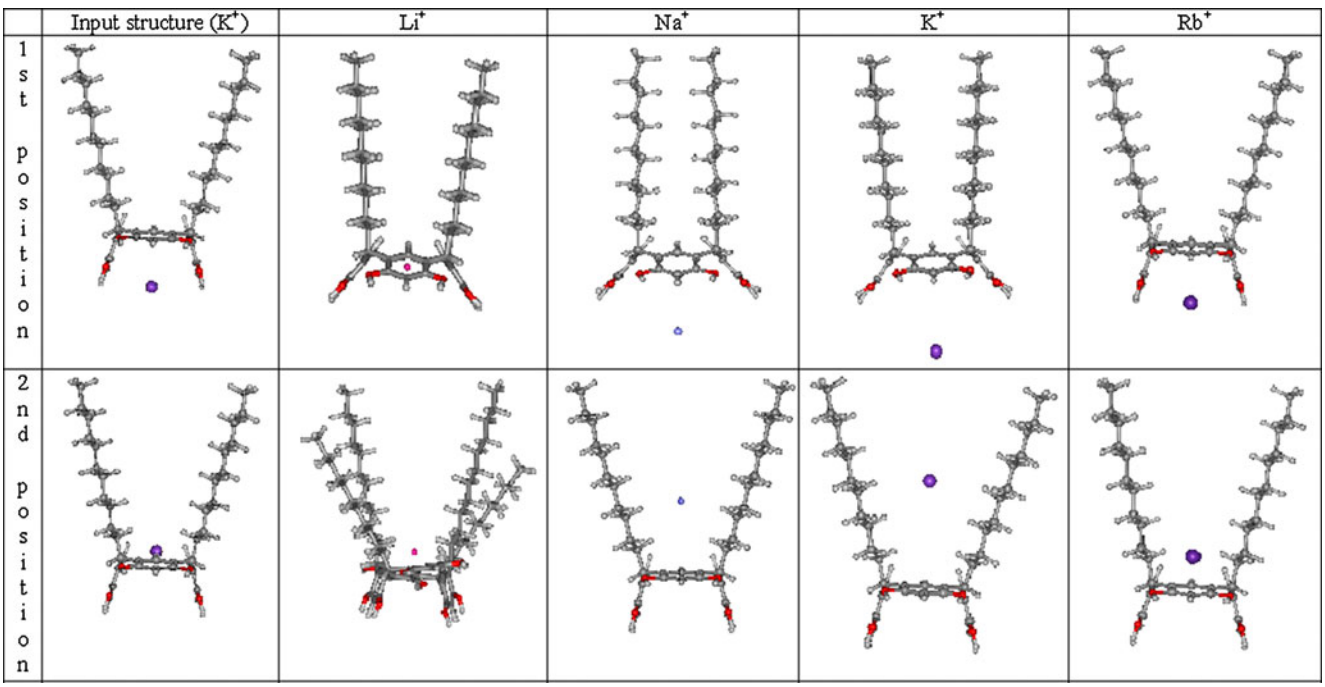

Fig. 10 The starting and eqilibrium positions of some alkali ions. Dynamic behavior

The charge functions of the front hydrogens have maxima at –11.25 Å, 16.75 Å and beyond the channel exit at 20.25 Å. Their minima can be found at –14.00 Å, 14.50 Å and beyond the exit at 18.50 Å. The charge function of the back hydrogens shows maxima and minima with opposite sign.

The interactions with the potassium complex are always stronger than the same with the sodium analogue. This is reflected in the higher system energy, in the more positive hydrogen charges (Fig. 9) and in the more negative oxygens (Fig. 8). The charge value extrema at –14.00 and 14.00 Å are identical with those found in case of the dehydrated alkali ions.

Summarizing up, according to our models, the investigated ion channels exhibit both attracting and repulsing potentials for the transported ion. In order to improve the ion conducting properties of the artificial ion channel, an auxiliary potential has to be introduced along the channel for carrying out the ion transport across the cell membrane.

Dynamic ion-channel interactions

The optimal location of different alkali ions in the ion channel is obviously characteristic and it forms the base of the selectivity of an ion channel. That is why the motion of different alkali ions were simulated where they tend to move along due to different attraction and repulsion effects of inner part of the artificial ion channel. In the frame of the possibilities of the Gaussian 98 program package [22] we investigated the effects of several alkali ions, namely, Li^+, Na^+, K^+ and Rb^+. Only a half channel, i.e., one TUR was investigated within which the optimal position of the studied ion could be characterized by potential energy minimum. Two different starting positions were chosen for the calculation of optimal locations of every ion in the input files, the optimizations started with these selected geometries. The first optimal position was found before the input slot of the channel at the –17.5 Å position along the channel axis (see Fig. 4). In the second case, the positioning of the ion was started at the maximal positive electrostatic potential along the channel axis, at the –13.0 Å position.

By comparing the results of the structure optimizations, the behavior of the studied alkali ions were found very different. Table 3 contains the most important data. By starting the optimization from the channel slot, the ions were driven along the channel axis in a very different way.

Lithium forms a very small ion. It moves a lot from the slot into the inner part of the channel, similarly it will move away for a longer distance to find the maximum place of the electrostatic potential. This ion exhibits a strong interaction with the channel environment, probably due to its high charge density. Its Mullikan charge exceeds +1.

The behavior of sodium ion in the artificial ion channel is absolutely different. Our calculations shows that the Na^+ ion will be repulsed outside form the slot and repulsed far from the place of the maximal electrostatic potential deep into the small potential part of the channel.

The interactions of potassium ion are very different again. One may expect that the larger ion will be attracted from the slot like the Na^+. However, just the opposite occurs. The K^+ penetrates from the slot very deeply into the inner part the channel as it became evident from the result of the second calculation (Fig. 10). This result explains the potassium-selectivity of the TUR channel over sodium (see also Refs. [19, 20]).

Regarding the rubidium ion, one can say, the effect of the relatively large size of the ion can be observed. The displacement of this ion is small according to results of both calculations. The space between the benzene rings seems relatively narrow for this ion. Its electrostatic repulsion is smaller inside the channel than for the other investigated ions. That could be the reason why Tanaka et al. [19] observed that rubidium ions blocked the transport of sodium ions through TUR channel.

Conclusions

The behavior of the alkali ions from lithium to potassium shows a definite trend in finding their position with minimum energy in our ion channel model, if the starting position of the ion is in the polar head of the TUR. This trend, however, breaks with the rubidium ion. The atomic-molecular structure of this molecular assembly – i.e., TUR embedded in phospholipid bilayer – and the motion of the different hydrated alkali ions toward the optimal minimal energy locations of the TUR explain the potassium selectivity of this artificial ion channel over sodium. It is also understandable why the rubidium ion can prevent sodium-transport through TUR channel. This trend is in line with experimental results (see [19, 20]).

The ultimate conclusion can be that TUR molecule estimates the ion transporting features of a natural, potassium selective ion channel quite well, thus it is a suitable model of ion transport across a natural Gramicidin-type ion channel.

Acknowledgments The authors would like to express their gratitude for the help of Prof. Reiner Saltzer (Institute of Analytical Chemistry, Dresden University of Technology). I. M-Z participated in this work as a former staff member of IR and Raman Laboratory, Chemical Research Center of the Hungarian Academy of Sciences, Budapest.

References

1. Hille B (2001) Ion channels of excitable membranes, 3rd edn. Sinauer Associates, Sunderland, MA, USA
2. Aidley DJ, Stanfield PR (1996) Ion channels: molecules in action. Cambridge University Press, Cambridge, UK

3. Kew JNC (2010) Davies CH (2010) Ion channels: from structure to function. Oxford University Press, Oxford, UK
4. Gillespie D, Eisenberg RS (2002) Physical descriptions of experimental selectivity measurements in ion channels. Eur Biophys J 31:454–466. doi:10.1007/s00249-002-0239-x
5. Hall LT, Hill CD, Cole JH, Städler B, Caruso F, Mulvaney P, Wrachtrup J, Hollenberg LCL (2010) Monitoring ion-channel function in real time through quantum decoherence. PNAS 107:18777–18782. doi:10.1073/pnas.1002562107
6. Siwy Z, Ausloos M, Ivanova K (2002) Correlation studies of open and closed state fluctuations in an ion channel: analysis of ion current through a large-conductance locust potassium channel. Phys Rev E 65:031907. doi:10.1103/PhysRevE.65.031907
7. Guidoni L, Carloni P (2002) Potassium permeation through the KcsA channel: a density functional study. Biochim Biophys Acta 1563:1–6. doi:10.1016/j.bpc.2006.04.008
8. Roux B (2002) Computational studies of the Gramicidin channel. Acc Chem Res 35:366–375. doi:10.1021/ar010028v
9. Grigorenko BL, Nemukhin AV, Topol IA, Burt SK (2002) Modeling of Biomolecular Systems with the Quantum Mechanical and Molecular Mechanical Method Based on the Effective Fragment Potential Technique: Proposal of Flexible Fragments. J Phys Chem A 106:10663–10672. doi:10.1021/jp026464w
10. Vogel C (2002) Modeling transport across biological membranes. Structural Studies Division MRC Laboratory of Molecular Biology, Hills Road, Cambridge. http://polaris.icmb.utexas.edu/people/cvogel/Dogs/mini1_gapjct.doc
11. Liu JL (2011) A quantum corrected Poisson-Nernst-Planck model for biological ion channels. www.nhcue.edu.tw/~jinnliu/proj/Device/2011QCPNP.pdf
12. Abad E, Reingruber J, Sansom MSP (2009) On a novel rate theory for transport in narrow ion channels and its application to the study of flux optimization via geometric effects. J Chem Phys 130 (055101):1–18. doi:10.1063/1.3077205
13. Poznanski RR, Bell J (2000) A dendritic cable model for the amplification of synaptic potentials by an ensemble average of persistent sodium channels. Math Biosci 166:101–121. doi:10.1016/S0025-5564(00)00031-6
14. Poznanski RR, Bell J (2000) Theoretical analysis of the amplification of synaptic potentials by small clusters of persistent sodium channels in dendrites. Math Biosci 166:123–147. doi:10.1016/S0025-5564(00)00032-8
15. Chen JL, Tsai CH, Chen YY (1995) The application of hidden markov model to the problem of ion channel modeling; National Science Council, NSC 84-2213-E-216-020
16. Ash WL, Zlomislic MR, Oloo EO, Tieleman DP (2004) Computer simulations of membrane proteins. Biochim Biophys Acta 1666:158–189. doi:10.1016/j.bbamem.2004.04.012
17. Tieleman DP, Biggin PC, Smith GR, Sansom MSP (2001) Simulation approaches to ion channel structure–function relationships. Q Rev Biophys 34:473–561. doi:10.1017/S0033583501003729
18. Bohmer V (1995) Calixarenes, macrocycles with (almost) unlimited possibilities. Angew Chem Int Ed Engl 34:713–745. doi:10.1002/anie.199507131
19. Tanaka Y, Kobuke Y, Sokabe M (1995) A non-peptidic ion channel with K^+ selectivity. Angew Chem Int Ed 34:693–694. doi:10.1002/anie.199506931
20. Chen WH, Nishikawa M, Tan SD, Yamamura M, Satake A, Kobuke Y (2004) Tetracyanoresorcin[4]arene ion channel shows pH dependent conductivity change. Chem Commun (Camb) 7:872–873. doi:10.1039/B312952G
21. Kulikov OV, Li R, Gokel GW (2009) A synthetic ion channel derived from a metallogallarene capsule that functions in phospholipid bilayers. Angew Chem Int Ed Engl 48:375–377. doi:10.1002/anie.200804099
22. Frisch MJ, Trucks GW, Schlegel HB, Scuseria GE, Robb MA, Cheeseman JR, Zakrzewski VG, Montgomery JA Jr, Stratmann RE, Burant JC, Dapprich S, Millam JM, Daniels AD, Kudin KN, Strain MC, Farkas O, Tomasi J, Barone V, Cossi MR, Cammi R, Mennucci B, Pomelli C, Adamo C, Clifford S, Ochterski J, Petersson GA, Ayala PY, Cui Q, Morokuma K, Malick DK, Rabuck AD, Raghavachari K, Foresman JB, Cioslowski J, Ortiz JV, Stefanov BB, Liu G, Liashenko A, Piskorz P, Komaromi I, Gomperts R, Martin RL, Fox DJ, Keith T, Al-Laham MA, Peng CY, Nanayakkara A, Gonzalez C, Challacombe M, Gill PMW, Johnson B, Chen W, Wong MW, Andres JL, Gonzalez C, Head-Gordon M, Replogle ES, Pople JA (1998) Gaussian 98, Revision A.3. Gaussian Inc, Pittsburgh, PA
23. Billes F, Mohammed-Ziegler I (2002) *Ab initio* equilibrium geometry and vibrational spectroscopic study of 25,26,27,28-tetrahydroxycalix[4]arene. Supramol Chem 14:451–459. doi:10.1080/10610270212491
24. Furer VL, Borisoglebskaya EI, Kovalenko VI (2005) Band intensity in the IR spectra and conformations of calix[4]arene and thiacalix[4]arene. Spectrochim Acta A 61:355–359. doi:10.1016/j.saa.2004.05.009
25. Backes AC, Schatz J, Siehl HU (2002) GIAO-DFT calculated and experimentally derived complexation-induced chemical shifts of calix[4]arene–solvent inclusion complexes. J Chem Soc -Perkin Trans 2:484–488. doi:10.1039/B110078P
26. Choe JI, Lee SH (2004) *Ab Initio* Study of the conformational isomers of tetraethyl and triethyl esters of calix[4]arene. B Kor Chem Soc 25:553–556. doi:10.5012/bkcs.2004.25.6.847
27. Mäkinen M, Jalkanen JP, Vainiotalo P (2002) Conformational properties and intramolecular hydrogen bonding of tetraethyl resorcarene: an *ab initio* study. Tetrahedron 58:8591–8596. doi:10.1016/S0040-4020(02)00863-3
28. Rempe SB, Pratt LR (2000). Ion hydration studies aimed at ion channel selectivity. Theor Chem Mol Phys T-12. Los Alamos. http://www.t12.lanl.gov/projects/rempe.pratt.00.pdf